Development/Plasticity/Repair

The Protein Kinase A Regulatory Subunit R1A (Prkar1a) Plays Critical Roles in Peripheral Nerve Development

Li Guo,[1] Audrey A. Lee,[2] Tilat A. Rizvi, Nancy Ratner,[1] and Lawrence S. Kirschner[2,3]

[1]Division of Experimental Hematology and Cancer Biology, Department of Pediatrics, Cincinnati Children's Hospital Medical Center, Cincinnati, Ohio 45229, [2]Department of Molecular, Virology, Immunology, and Medical Genetics, and [3]Division of Endocrinology, Diabetes, and Metabolism, Department of Internal Medicine The Ohio State University, Columbus, Ohio 43210

Signaling through cAMP has been implicated in Schwann cell (SC) proliferation and myelination, but the signaling pathway components downstream of cAMP required for SC function remain unknown. Protein kinase A (PKA) is a potential downstream effector of cAMP. Here, we induced loss of *Prkar1a*, the gene encoding the type 1A regulatory subunit of PKA, in SC to study its role in nerve development; loss of Prkar1a is predicted to elevate PKA activity. Conditional *Prkar1a* knock-out in mouse SC (Prkar1a-SCKO) resulted in a dramatic and persistent axonal sorting defect, and unexpectedly decreased SC proliferation in Prkar1a-SCKO nerves *in vivo*. Effects were cell autonomous as they were recapitulated *in vitro* in Prkar1a-SCKO SC, which showed elevated PKA activity. In the few SCs sorted into 1:1 relationships with axons *in vivo*, SC myelination was premature in Prkar1a-SCKO nerves, correlating with global increase in the cAMP-regulated transcription factor Oct-6 and expression of myelin basic protein. These data reveal a previously unknown role of PKA in axon sorting, an unexpected inhibitory role of PKA on SC cell proliferation *in vivo* and define the importance of *Prkar1a* in peripheral nerve development.

Introduction

Schwann cells (SCs) are glial cells of the peripheral nervous system (PNS). During development, mouse neural crest cells differentiate into SC precursors (SCPs) at embryonic day (E) 12–13, and into immature SCs at E15–16 (Jessen and Mirsky, 1997; Woodhoo and Sommer, 2008). Immature SCs segregate progressively smaller groups of axons by extending processes into axon bundles in a process called radial sorting. SCPs and immature SCs proliferate rapidly, with the postnatal onset of myelination by SCs associating with single large diameter axons correlating with cell-cycle exit (Stewart et al., 1993; Jessen and Mirsky, 2005). The transcription factors Krox-20, Oct-6 (SCIP or Pou3f1), and nuclear factor κ B (NF-κB) are crucial for SC proliferation and myelination (Pereira et al., 2012).

cAMP has been implicated as an important second messenger regulating SC proliferation and myelination (Jessen and Mirsky, 1991; Morgan et al., 1991). *In vitro*, cAMP enhances mitogen-dependent SC proliferation (Davis and Stroobant, 1990; Stewart et al., 1991; Jung-Testas et al., 1993; Kim et al., 1997; Monje et al., 2006). In rat SCs, high cAMP increases expression of myelin genes (Sobue et al., 1986). In mouse SCs, increasing levels of cAMP switches neuregulin 1 (NRG1) from a proliferative signal

to a myelin differentiation signal (Arthur-Farraj et al., 2011). Furthermore, *in vivo Gpr126* is essential to initiate SC myelination through cAMP (Monk et al., 2009, 2011), and low cAMP levels in Rac1 mutant SCs result in the absence of SC myelin sheaths *in vivo* (Guo et al., 2012).

The best known downstream effector of cAMP is PKA. PKA-mediated phosphorylation of the NF-κB p65 subunit is required for myelination in SC-neuron cocultures and a peak of PKA activity in the sciatic nerve occurs around the onset of myelination (Yoon et al., 2008). PKA is composed of two regulatory (RIα- or RIβ-, RIIα- or RIIβ-) and two catalytic subunits (Skalhegg and Tasken, 2000; Taylor et al., 2005). cAMP binding to regulatory subunits results in release of catalytic subunits, which then phosphorylate PKA substrates (Barradeau et al., 2002). Loss of regulatory subunits is predicted to increase PKA activity (Amieux et al., 2002; Cheng et al., 2008), and this was demonstrated *in vivo* and *in vitro* (Kirschner, 2009). *Prkar1a* encodes the PKA regulatory subunit type IA (RIα), an important effector of cAMP signaling in most cells and *Prkar1a* gene is mutated in Carney Complex, a schwannoma predisposition syndrome (Bossis and Stratakis, 2004).

Despite significant *in vitro* data supporting the importance of cAMP in promoting SC proliferation and myelination, effects of PKA signaling on peripheral nerve have not been analyzed *in vivo* and relevant PKA subunits have not been defined. We induced *Prkar1a* loss at the SCP stage of development, resulting in a dramatic and persistent axonal sorting defect, and decreased SC proliferation in Prkar1a-SCKO nerves. In *Prkar1a* null SCs sorted into 1:1 relationships with axons *in vivo*, myelination began prematurely, correlating with an increase in a cAMP-regulated transcription factor, SCIP/Oct-6, expression and increased myelin basic protein (MBP) expression.

Materials and Methods

Generation of DhhCre directed conditional Prkar1a knock-out mice. *Prkar1a$^{flox/flox}$* (Kirschner et al., 2005) mice were bred to *DhhCre* mice (Jaegle et al., 2003; Wu et al., 2008) to obtain *DhhCre+; Prkar1a$^{flox/flox}$* (Prkar1a-SCKO) mice. Littermate *DhhCre+; Prkar1a flox/+* mice were used as controls. A *lox-STOP-lox RFP* allele (lslRFP) was used as a Cre recombination reporter (Madisen et al., 2010). The genotypes of *Dhh* and *Prkar1a* alleles for all of the mice in our experiments were analyzed by PCR. The primers for *DhhCre* genotyping were 5′-GCGGTCTGGCAG TAAAAACTATC-3′ (forward) and 5′-GTGAAACAGCATTGCTGTCAC TT-3′ (reverse). The primers for *Prkar1a* genotyping were 5′-GCAGGC GAGCTATTAGTTTA-3′ (forward) and 5′-CATCCATCTCCTATCCCC TTT-3′ (reverse). Primer 5′-CAAGCTAGCTTGGCTGGACGTA-3′ (forward) was used to identify the *Prkar1a* knock-out band. All mouse crosses were performed in a mixed genetic background, consisting primarily of the *FVB, C57 Bl/6,* and *129* strains. All animal experiments were conducted in mice of both sexes.

Electron microscopy. Mice were anesthetized and fixed with electron microscopy fixation solution (3% paraformaldehyde and 3% glutaraldehyde in PBS, pH 7.4–7.6). Sciatic nerves of wild-type and mutant mice were dissected, postfixed, osmicated, embedded, and sectioned. The photographs of toluidine blue stained semithin sections (1 μM) were taken by bright-field microscopy. High-magnification pictures of ultrathin sections stained with uranyl acetate and lead citrate were taken using a Hitachi H-7600 transmission electron microscope.

Western blots. Sciatic nerve tissue was homogenized using a TissueRuptor (Qiagen) or cultured cells were lysed in ice-cold lysis buffer (20 mM NaPO$_4$, 150 mM NaCl, 2 mM MgCl2, 0.1% Nonidet P-40, 10% glycerol, 10 mM sodium fluoride, 0.1 mM sodium orthovanadate, 10 mM sodium pyrophosphate, 10 nM okadaic acid, 1 mM dithiothreitol, 10 μg/ml leupeptin, 10 μg/ml aprotinin, 10 μg/ml pepstatin, 10 μg/ml tosyl-L-phenylalanine chloromethyl ketone, and 10 μg/ml N α-tosyl-L-lysine chloromethyl ketone). Homogenates were centrifuged at 6000 $\times$ *g* for 10 min and protein extract supernatants were collected. Protein concentration was measured on a spectrophotometer using a Bio-Rad DC Protein Assay Kit. Equal amounts of protein were fractionated by 4–20% SDS-PAGE (NuStep) and transferred to PVDF membrane. Membranes were incubated with primary antibodies followed by appropriate secondary antibodies, and developed by GE Healthcare ECL Detection Reagents. The following primary antibodies were used: Prkar1a (Cell Signaling Technology, 1:1000), ErbB3 (Santa Cruz Biotechnology, 1:500), P-AKT (Cell Signaling Technology, 1:1000), Akt (Cell Signaling Technology, 1:1000), P-Erk1/2 (Cell Signaling Technology, 1:1000), Erk1/2 (Cell Signaling Technology, 1:1000), Krox20 (Abcam, 1:500), Pmp22 (Abcam, 1:10,000), MBP (Calbiochem, 1:1000)c and β-actin (Cell Signaling Technology, 1:10,000). Anti-rabbit and anti-mouse HRP-conjugated secondary antibodies (1:5000) were purchased from Bio-Rad.

Immunohistochemistry. Sciatic nerves were dissected and fixed in 4% paraformaldehyde (PFA) overnight. For cryostat sections, fixed sciatic nerves were incubated in 20% sucrose buffer and then frozen in OCT compound (Sakura). Frozen blocks were cut into 6–8 μm frozen sections using a Leica Cryostat. For paraffin sections, fixed sciatic nerves were incubated in 70% ethanol then processed in paraffin wax. Paraffin blocks were cut into 4 μm paraffin sections. For staining, paraffin sections were deparaffinized and rehydrated before staining. Sodium citrate buffer (pH 6.0) was used for antigen unmasking. Frozen sections were incubated with 4% PFA for 20 min at room temperature then washed in PBS and permeabilized with 0.3% Triton X-100 in PBS when necessary. Paraffin or frozen sections were blocked for 1 h with blocking buffer (10% serum in PBS) and incubated with primary antibody at 4°C overnight. The next day, sections were washed with PBS and incubated in Alexa Fluor 488-conjugated secondary antibodies (Jackson ImmunoResearch, 1:400) for 1 h at room temperature. To visualize nuclei, sections were stained with DAPI for 10 min, and then washed with PBS and mounted in Fluoromount G (Electron Microscopy Sciences). ABC avidin/biotin method was used for Ki67 staining in paraffin section. The section was counterstained with hematoxylin (blue) to visualize nuclei. The following primary antibodies were used: Ki67 (Ventana); MBP (Aves Labs); Oct-6 (Santa Cruz Biotechnology); neurofilament (Developmen-

tal Studies Hybridoma Bank). All the images were acquired using a fluorescence microscope with 10$\times$/0.4 or 40$\times$/0.6 objectives (Carl Zeiss). Acquisition software ImageJ was used.

Brdu incorporation and TUNEL assay. Pregnant mice were injected with bromodeoxyuridine (BrdU, Sigma-Aldrich; 50 mg /kg body weight) three times at 2 h intervals. Twenty-four hours later, mice were killed and sciatic nerves were dissected from pups at P0 or embryos at E18 and E19. Sciatic nerves were fixed with 4% PFA overnight then processed into 6 μm frozen sections. Sections were stained with anti-Brdu antibody (Accurate Chemical, 1:500). Nuclei were stained with DAPI. BrdU-labeled cells and the DAPI nuclei were counted to define percentages of proliferating cells. TUNEL staining of control and mutant nerves were conducted by using an In Situ Cell Death Detection Kit, Fluorescein (Roche).

Schwann cell culture. Primary mouse SC cultures were obtained from postnatal day (P) 30 sciatic nerves. Sciatic nerves were sterilely dissected from killed P30 mice and cultured at 37°C, 7.5% CO$_2$ in DMEM medium (Invitrogen) supplemented with 10% fetal bovine serum (Gemini Bio-Products), 1% penicillin-streptomycin (Fisher Scientific), forskolin (2 μM, Calbiochem), and β-heregulin (HRG, 10 ng/ml, R&D Systems). Pretreatment medium was replaced every 2 d. After 6–9 d nerves were incubated in dissociation medium [Leibovitz medium (Invitrogen) containing collagenase type I (130 U/ml, Worthington Biochemical Corporation), dispase II (2.5 mg/ml, Roche Diagnostics), gentamycin (50 μg/ml, Lonza) and fungizone (2.5 μg/ml, Invitrogen)] for 3 h at 37°C. Cells were dissociated using a narrowed Pasteur pipette and were then centrifuged for 5 min at 1000 rpm. Cells were resuspended in DMEM/ F-12 medium (Invitrogen) supplemented with N2 supplement solution (Invitrogen), forskolin (2 μM, Calbiochem), β-heregulin (HRG; 10 ng/ml), gentamycin (50 μg/ml, Lonza), and fungizone (2.5 μg/ml, Invitrogen). Cells were plated on poly-L-lysine (Sigma-Aldrich) and laminin-coated (BD Bioscience) plates and incubated at 37°C, 7.5% CO$_2$. Medium was changed every 3 d and the cells were passaged when confluent. Cells were used at passages 0–1.

Adenovirus infection and immunostaining. Cultured *Prkar1a $^{flox/flox}$; lslRFP* SCs at 50% confluence were treated with adenovirus-expressing Cre recombinase. The Crude adenovirus lysates were added in serum free medium (1:1) and incubated with cells for 6 h. Cells were washed with PBS, and then cultured in SC culture medium. Adenovirus-expressing green fluorescence protein (GFP) was used as a control. Twenty-four hours after adenovirus infection, RFP was detectable in adeno-Cre infected *Prkar1a $^{flox/flox}$; lslRFP* SCs. These cells were cultured for up to 6 d and the cell growth and morphology were monitored by light microscopy. Cells were fixed and stained with antibodies recognizing the SC markers S100β (Dako) and P75NTR (Millipore).

PKA activity assay. Passage one SCs were infected with GFP or Cre adenovirus. Forty-eight hours after infection cells were extracted for 10 min in ice-cold lysis buffer (20 mM 3-morpholinopropanesulfonic acid, 50 mM β-glycerolphosphate, 50 mM sodium fluoride, 1 mM sodium vanadate, 5 mM EGTA, 2 mM EDTA, 1% NP40, 1 mM dithiothreitol, 1 mM benzamidine, 1 mM phenylmethane-sulfonylfluoride, and 10 μg/ml leupeptin and aprotinin). Supernatants were collected by centrifugation at 150,000 $\times$ *g* for 30 min at 4°C. Concentration of supernatant protein was measured by a protein assay kit (Bio-Rad). PKA activity was measured with a kinase assay kit (ENZO Life Science, catalog #ADI-EKS-390A) using microplate wells precoated with a PKA substrate, according to the manufacture's protocol, with the addition of a wash step after stopping the reactions. The absorbance in reactions was measured at 450 nm in a microplate reader. Absorbance was divided by total protein (μg) per sample and the data represented as relative PKA activity.

Morphometric quantification and statistical analysis. Total cell numbers in nerve cross sections were counted in semithin sections. Morphometric measurements of axonal sorting and myelination were performed in electron microscopic images of the nerve cross sections. A cell-counter plugin from ImageJ software was used to analyze the number of one-to-one myelinated axons, and the axon number in each axonal bundle. Statistical significance was determined between two individual samples with the Student's *t* test. For multiple comparisons, one-way ANOVA followed by Tukey's *post hoc* test was used. Significance was denoted as *$p < 0.05$, **$p < 0.01$, or ***$p < 0.001$.
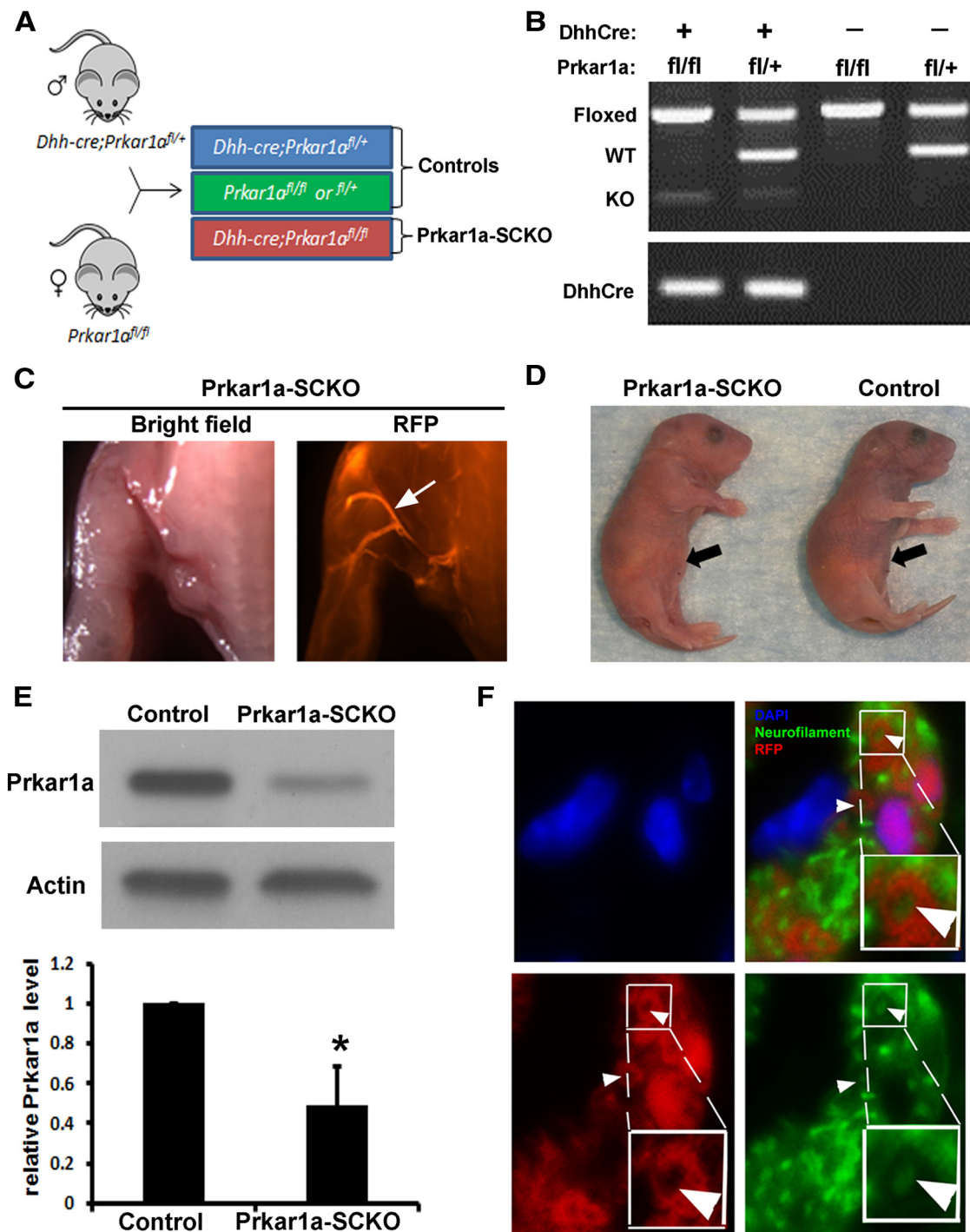
Figure 1. Generation and characterization of Prkar1a-SCKO mice. ***A***, Mating scheme: fl, floxed conditional allele; +, wild-type (WT) allele. ***B***, Genotyping. DhhCre, *Prkar1a* WT (+), floxed (fl), and deletion (KO) alleles in wild-type and Prkar1a-SCKO tails. The KO allele only appears in mice carrying DhhCre. ***C***, Gross hindlimb of mutant pup, with RFP expression in Prkar1a-SCKO nerves (arrow) after Cre-mediated recombination. ***D***, Prkar1a-SCKO mice are phenotypically indistinguishable from WT littermates. Pups have milk in their bellies (arrows). ***E***, Western blot showing reduction of Prkar1a protein levels in P0 mutant sciatic nerve lysates compared with wild-type nerves. For analysis, n = independent blots from three nerves lysates for each genotype (*$p < 0.05$, Student's t test). ***F***, Cross sections of Prkar1a-SCKO sciatic nerves at P0 stained with an axon marker, neurofilament (green). RFP (red) is expressed in Prkar1a-SCKO SCs after Cre-mediated recombination. Axons were not RFP-positive (arrowhead). Nuclei are visualized by DAPI (blue).

Results

Conditional knock-out of Prkar1a in SCs *in vivo*

To analyze the role of *Prkar1a* in SCs *in vivo*, *Prkar1a* conditional knock-out mice (Prkar1a-SCKO) were generated using the Cre recombinase-LoxP system under the control of the *desert hedge-hog* (Dhh) gene. In these mice, Dhh activates Cre recombinase

expression in SCPs at day E12.5 (Jaegle et al., 2003; Wu et al., 2008). *Prkar1a*^{flox/flox} mice were bred with *Dhh-Cre Prkar1a*^{+/−} mice (Fig. 1A). The *Prkar1a* knock-out alleles were confirmed by PCR (Fig. 1B). We introduced a lox-STOP-lox red fluorescent protein (lslRFP) allele as a Cre recombination reporter (Madisen et al., 2010). RFP was expressed in Cre-positive peripheral nerves
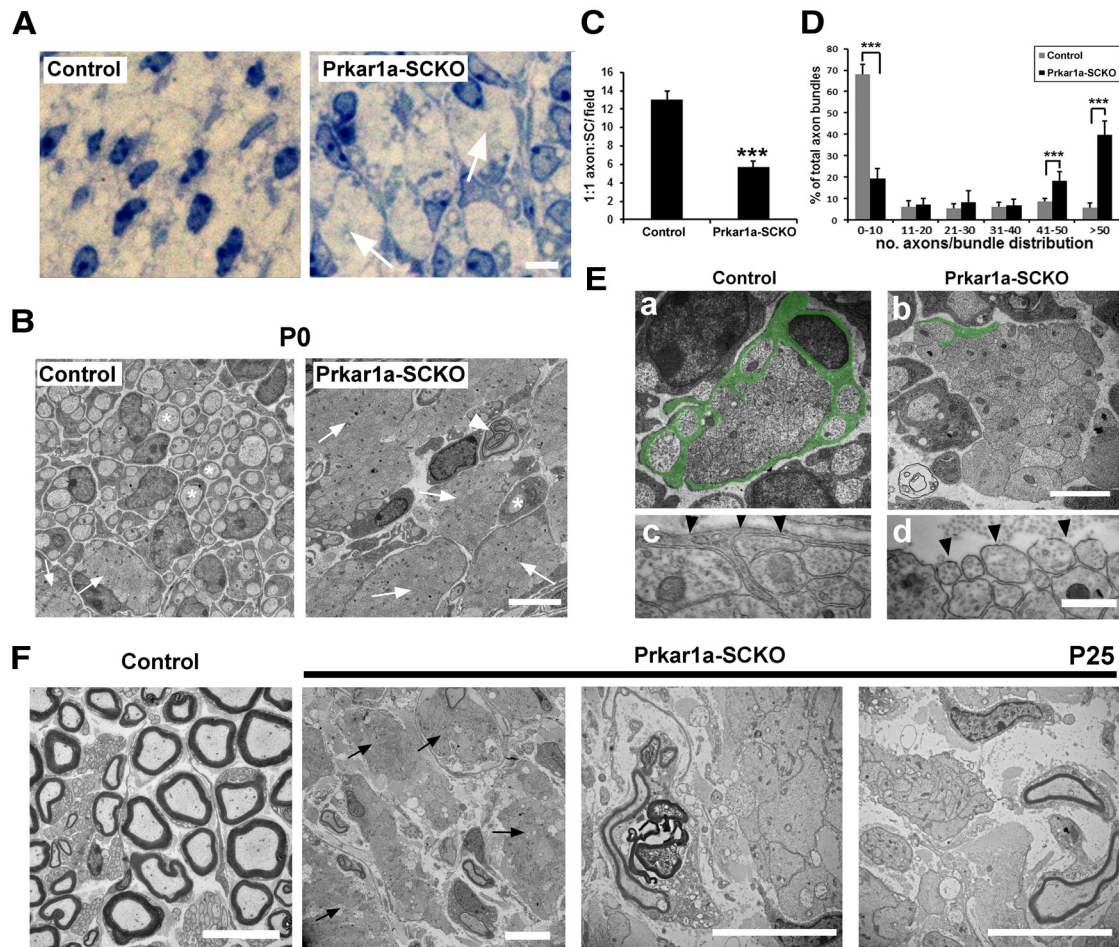
Figure 2. Axonal sorting defects in Prkar1a-SCKO sciatic nerve. ***A***, Semithin cross sections of Prkar1a-SCKO sciatic nerves at P0. ***B***, Electron microscopy (EM) analysis of control and Prkar1a-SCKO sciatic nerves cross-sections at P0. Unsorted axonal bundles (arrow) and SC:axon in 1:1 relationships (asterisk) are denoted. ***C***, Decrease in the number of 1:1 SC-axon bundles in Prkar1a-SCKO sciatic nerves. ***D***, Axon bundles in Prkar1a-SCKO sciatic nerves contain more axons per bundle. ***C, D***, For each genotype, $n = 4$ mice (***$p < 0.001$, Student's t test). Error bars indicate $\pm$ SEM. ***E***, EM of axonal bundles from control (***Ea, Ec***) and Prkar1a-SCKO (***Eb, Ed***) sciatic nerves at P0. SC processes are highlighted with artificial color (green). ***Ec, Ed***, High-magnification micrographs of the edges (arrowheads) of axonal bundles from control (***Ec***) and Prkar1a-SCKO sciatic nerves (***Ed***). ***F***, EM analysis of sciatic nerves cross-sections from control and a rare surviving Prkar1a-SCKO mouse at P25. Unsorted axon bundles (arrows) were present in this P25 Prkar1a-SCKO mouse. Scale bars: ***A, B***, 5 μM; (in ***Eb***) ***Ea, Eb***, 2 μM; (in ***Ed***), ***Ec, Ed***, 500 nM; ***F***, 10 μM.

(Fig. 1C). Conditional knock-out of *Prkar1a* beginning in SCPs did not cause embryonic lethality or obvious developmental defects in pups at birth (Fig. 1D). More than 90% of Prkar1a-SCKO mice died within 48 h after birth. Of 20 litters, only three mice survived to weaning age, and all three were severely runted and exhibited seizure-like activity requiring euthanasia by day 25. The cause of death remains unknown; milk was present in pup stomachs, and pups appeared to breathe normally. Reduction of Prkar1a protein expression in the sciatic nerves of mutant pups was verified by Western blot (Fig. 1E). Residual Prkar1a protein in mutant nerves is likely caused by its expression in fibroblasts and/or axons. RFP expression was present in SCs but not in neurofilament stained axons (Fig. 1F), consistent with a previous study showing that DhhCre is expressed in SCs and satellite cells but not neurons in dorsal root ganglia (Williams et al., 2008).

Radial sorting defects in Prkar1a-SCKO sciatic nerves
Prkar1a-SCKO sciatic nerves were compared with control nerves in semithin plastic cross sections. At E18 (data not shown) and at P0, large abnormal axon bundles were observed in Prkar1a-SCKO sciatic nerves (Fig. 2A). By electron microscopy, in control nerves many axons had already formed 1:1 relationships with SC. In contrast, numerous axonal bundles

containing large numbers of axons were observed in Prkar1a-SCKO sciatic nerves at P0 (Fig. 2B). SC nuclei penetrated axon bundles in control nerves, but in Prkar1a-SCKO nerves SC nuclei remained outside axon bundles, a characteristic of earlier stages of nerve development. Quantification confirmed a sorting defect; the number of SCs in 1:1 relationship with axons was significantly decreased in Prkar1a-SCKO sciatic nerves at P0 (Fig. 2C), and 70% of axon bundles in Prkar1a-SCKO sciatic nerves contained >20 axons within each bundle (Fig. 2D). Unsorted axonal bundles persisted through postnatal day 25 in sciatic nerves from a rare surviving Prkar1a-SCKO mouse (Fig. 2F), confirming a radial sorting defect rather than a maturation delay in Prkar1a-SCKO SCs.

We observed another abnormality in electron micrographs of Prkar1a-SCKO sciatic nerves. In axon bundles of control nerves, SC processes surround axons, isolating individual axons from the environment. However, Prkar1a-SCKO SCs failed to surround axon bundles (Fig. 2E). Thus, axons in Prkar1a-SCKO nerves were largely exposed to the environment and were in contact with endoneurial collagen (Fig. 2E). This observation suggests that SCs fail to extend normal processes in Prkar1a-SCKO nerves *in vivo*.
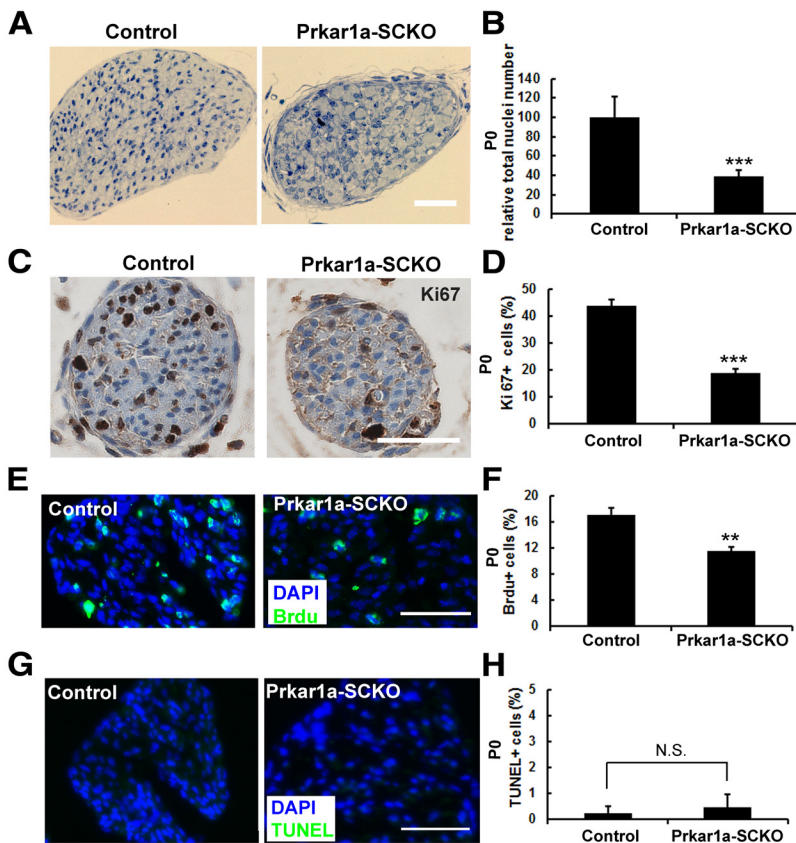
Figure 3. Reduced proliferation in Prkar1a-SCKO sciatic nerves. ***A***, Semithin cross sections. ***B***, Nuclei numbers in Prkar1a-SCKO sciatic nerves are significantly decreased at P0. ***C***, Paraffin cross sections from control and Prkar1a-SCKO nerve stained with Ki67; DAB was used as the chromogen (brown). The section was counterstained with hematoxylin (blue) to visualize nuclei. ***D***, The percentage of Ki67-positive cells is significantly decreased in Prkar1a-SCKO nerves. ***E***, Cross sections from control and Prkar1a-SCKO nerve stained with anti-BrdU. ***F***, Significant increases in percentage of BrdU+ cells in Prkar1a-SCKO nerves. ***G***, Paraffin cross sections from control and Prkar1a-SCKO nerve stained with TUNEL. ***H***, No difference in percentage of TUNEL+ cells in control and Prkar1a-SCKO nerves. For each genotype, $n = 4$ mice (**$p < 0.01$, ***$p < 0.001$, Student's t test). Error bars indicate ± SEM. Scale bars, 50 μm.

Prkar1a knock-out inhibits SC proliferation

SCs proliferate extensively during radial sorting to match SC numbers to numbers of axons to be ensheathed and/or myelinated. Radial sorting abnormalities in Prkar1a-SCKO nerves correlated with deficiencies in the number of SCs. Nuclei numbers in semithin cross sections of Prkar1a-SCKO sciatic nerves were significantly decreased compared with control sciatic nerves (Fig. 3*A*,*B*). Decreased proliferation or increased cell death could underlie decreased cell numbers in Prkar1a-SCKO nerves. Thus, we analyzed SC proliferation, and found less Ki67 staining in Prkar1a-SCKO nerve cross sections compared with wild-type nerve (Fig. 3*C*). The percentage of Ki67-positive cells (those in the cell cycle) was significantly decreased in Prkar1a-SCKO nerves at P0 (Fig. 3*D*). Reduced proliferation was confirmed by the decreased percentage of Brdu-positive cells (monitoring entry into S-phase of the cell cycle) in Prkar1a-SCKO nerves (Fig. 3*E*,*F*). In contrast, apoptotic cell death was unaffected by Prkar1a knock-out; there was no difference in percentage of TUNEL+ cells in control versus Prkar1a-SCKO nerves (Fig. 3*G*,*H*). Thus, radial sorting impairment in Prkar1a-SCKO correlates with reduced SC proliferation, and insufficient available cells to complete radial sorting in the absence of Prkar1a. This mirrors prior data showing decreased proliferation during organogenesis in a cardiac-specific KO of Prkar1a (Yin et al., 2008).

The onset of myelination is earlier in Prkar1a-SCKO sciatic nerves

In addition to axonal sorting defects in Prkar1a-SCKO sciatic nerves, myelin sheaths formed early in those SCs in 1:1 relationship with axons. At E18 in control nerves the few myelinating SCs present have loose uncompact myelin, whereas mutant SCs already had compact myelin (Fig. 4*A*). Quantification showed that there was a significant increase in myelinated fibers in E18–P0 Prkar1a-SCKO sciatic nerves compared with wild-type controls (Fig. 4*D*). Myelination in SCs is controlled by transcription factors, including Oct6, which initiates the transition from ensheathing, promyelinating SCs to myelinating cells; cAMP regulates Oct6 expression in SCs (Monuki et al., 1989). We reasoned that if cAMP/PKA signaling was increased in Prkar1a null SCs, this might upregulate Oct6 expression. Indeed, we detected a dramatic increase of Oct6 expression in most or all SCs in Prkar1a-SCKO sciatic nerves compared with control nerves at E18 (Fig. 4*B*), suggesting that Prkar1a is important to time the onset of myelination. Consistent with this finding, expression of a myelin marker, MBP, was increased in scattered cells, likely those in 1:1 relationships with axons, in Prkar1a-SCKO sciatic nerves at E18 compared with control sciatic nerves (Fig. 4*C*). Western blots show that MBP and peripheral myelin protein 22 (PMP22) were increased, whereas Krox20 expression was slightly decreased in Prkar1a-SCKO sciatic nerves (Fig. 4*E*). However, although expression of MBP was accelerated in Prkar1a-SCKO nerves, and few myelin sheaths formed early in those SCs in 1:1 relationship with axons in Prkar1a-SCKO sciatic nerves, this did not translate into presence of large numbers of myelinated fibers in a rare Prkar1a-SCKO nerve analyzed at P25 (Fig. 2*F*). The altered SC differentiation status (Oct6+;MBP− or Oct6+;MBP+) may contribute to the failure of axon sorting and decrease in cell proliferation.

The failure to ensheath axons might be responsible, at least in part, for the observed decreased SC proliferation. Axons normally stimulate SC proliferation via ErbB2/ErbB3 receptors that activate PI3K and MAPK signaling. Total ErbB3 expression and phosphorylation of Akt and Erk1/2 were reduced in Prkar1a-SCKO sciatic nerves (Fig. 4*E*), consistent with a failure of axon-mediated proliferation in Prkar1a-SCKO.

Cell autonomous reduced cell growth and abnormal cell morphology in Prkar1a-SCKO SCs *in vitro*

We cultured primary SCs from P30 sciatic nerves from *Prkar1a*^{*flox/flox*}; *lslRFP* mice to further define cell autonomous effects of *Prkar1a*. We used Cre adenovirus to infect SC and knock-out *Prkar1a in vitro*; control cells were infected with adenovirus encoding GFP. RFP was expressed by 24 h after adeno-Cre infection in *Prkar1a*^{*flox/flox*}; *lslRFP* SCs, whereas control adenovirus infected GFP-expressing cells were green (Fig. 5*A*). Western
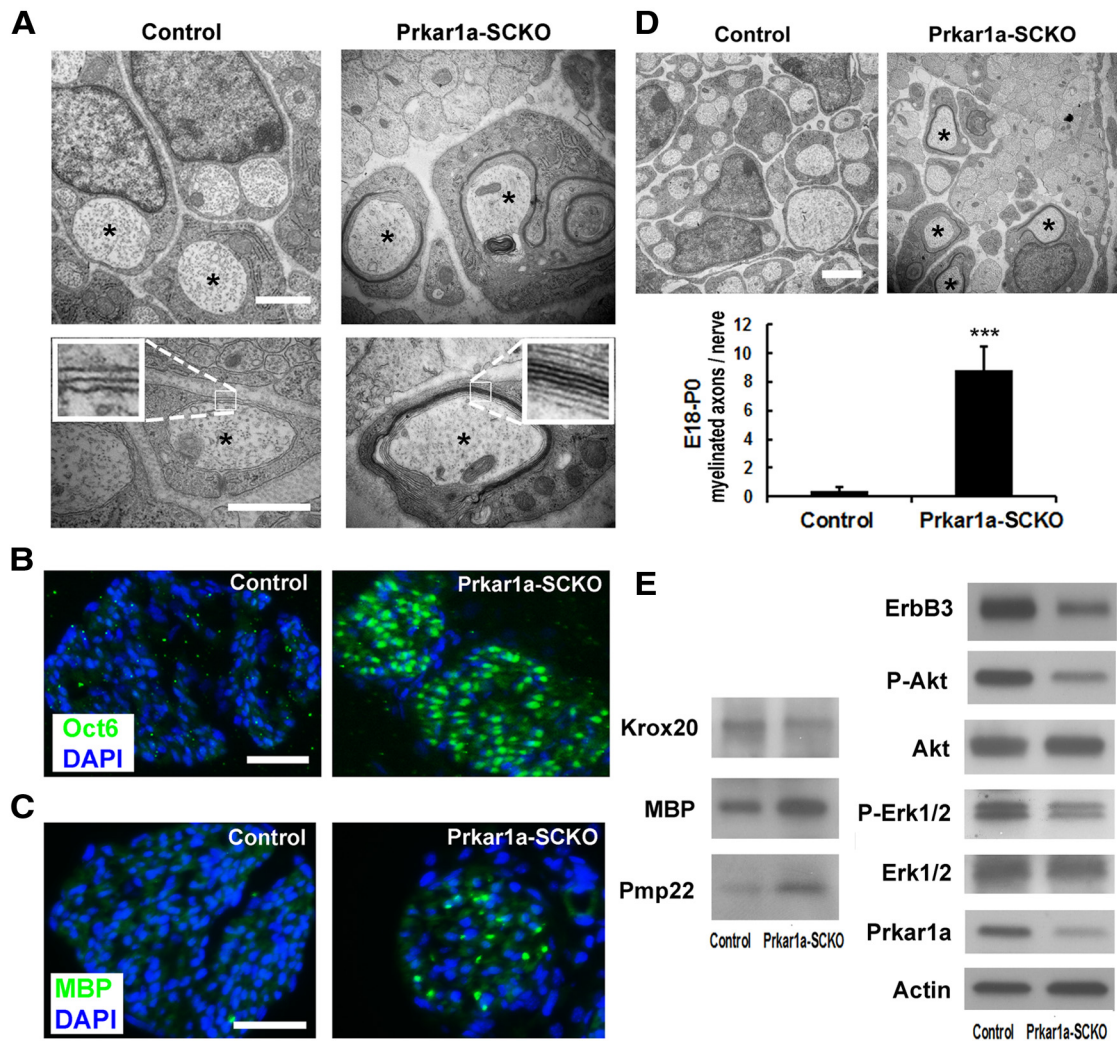
Figure 4. The onset of myelination is early in Prkar1a-SCKO sciatic nerves. **A**, EM shows 1:1 SC-axon relations (asterisks) in control and Prkar1a-SCKO sciatic nerves at E18. Bottom, more myelin wraps were present in Prkar1a-SCKO sciatic nerves. **B**, Oct6 expression was increased in Prkar1a-SCKO sciatic nerves stained with anti-Oct6. **C**, MBP expression was increased in E18 Prkar1a-SCKO sciatic nerves. **D**, EM shows myelinated axons (asterisks) in Prkar1a-SCKO sciatic nerves at P0. There was a significant increase in myelinated axons in E18–P0 Prkar1a-SCKO nerves. For each genotype, $n = 6$ mice at E18–P0 (***$p < 0.001$, Student's t test). Error bars indicate $\pm$ SEM. **E**, MBP and Pmp22 expression were increased, whereas Krox20 was slightly decreased in Prkar1a-SCKO sciatic nerve lysates. Total ErbB3, P-Akt, and P-Erk1/2 were decreased in Prkar1a-SCKO sciatic nerve lysates by Western blot ($n = 3$). β-Actin was used as a loading control. Scale bars: **A**, 1 μM; **B**, **C**, 25 μM; **D**, 2 μM.

blots confirmed the absence of Prkar1a protein 2 d after adeno-Cre infection (Fig. 5B). To test whether PKA activity is altered in Prkar1a-KO SCs, we measured PKA activity by a kinase assay 2 d after adenovirus infection. Basal PKA activity was increased two-fold in Prkar1a-KO SCs compared with GFP infected control SCs (Fig. 5C); a similar two-fold increase in PKA activity was observed after forskolin stimulation in Prkar1a-KO SCs compared with GFP infected control SCs (data not shown). We monitored cells for up to 6 d after adeno-Cre infection. Consistent with inhibition of proliferation in Prkar1a-SCKO nerves *in vivo*, numbers of cells in Prkar1a knock-out SC cultures decreased significantly compared with control SC cultures (Fig. 5D,E). The Prkar1a cells detached rapidly over time after infection, but there was no significant apoptosis as measured by cleaved caspase 3 (data not shown), supporting the idea that cells die by anoikis.

Cell morphology was also changed by Prkar1a knock-out in SC *in vitro* (Fig. 5F). Wild-type SCs normally extend two long processes and develop bipolar morphology in culture. Many Prkar1a knock-out SCs had multiple processes and formed nu-

merous branches (Fig. 5F). The cells with abnormal morphology in Prkar1a knock-out culture were SCs, as confirmed by staining with antibodies recognizing SC markers S100β and P75NTR (Fig. 5G).

The absence of Prkar1a regulatory subunits resulted in high PKA activity *in vitro*. We added the PKA inhibitor PKI 12 h after adeno-Cre infection to SC cultures, which decreased the occurrence of abnormal multiple processes (Fig. 5H). In addition, Prkar1a knock-out SCs formed fewer lamellipodia compared with control cells (Fig. 5I).

Discussion

Despite significant *in vitro* data supporting the importance of cAMP in promoting SC proliferation and myelination (Jessen and Mirsky, 1991; Morgan et al., 1991), effects of PKA signaling on SC proliferation had not been analyzed *in vivo*. Here, we studied the *in vivo* role of PKA signaling in SC using a new mouse model in which Prkar1a is lost beginning at the SCPs stage of development. Conditional *Prkar1a* knock-out resulted in a dramatic and persistent axonal sorting defect, and unexpectedly de-
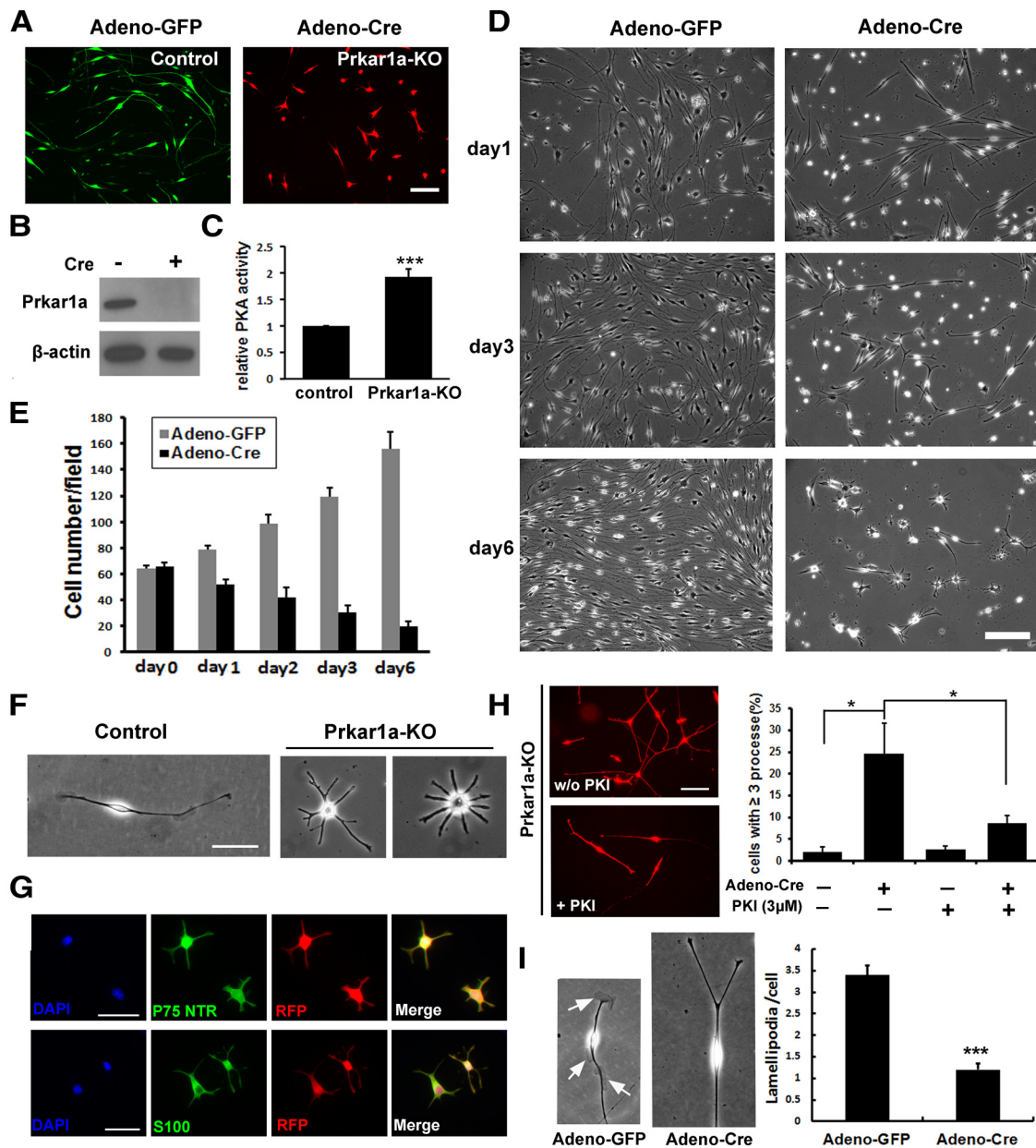
Figure 5. Prkar1a knock-out affects SC morphology. ***A***, Cultured primary SCs from P30 sciatic nerves from *Prkar1a^{loxp/loxp}*; *IslRFP* mice. RFP was expressed by 24 h after adeno-cre infection in Prkar1a-KO SCs, whereas control adenovirus infected GFP-expressing cells were green. ***B***, Prkar1a expression was reduced in Cre adenovirus infected SCs compared with GFP infected SCs (2 d after infection) by Western blot. β-Actin was used as a loading control. ***C***, PKA activity was significantly increased in Prkar1a-KO SCs. $n = 3$ independent experiments done in duplicate. ***D***, SC cultures were monitored for 6 d after infection. ***E***, Cell numbers in Prkar1a-KO SCs were significant reduced compared with control SCs. $n = 30$ fields from three independent experiments. ***F***, Phase micrographs of control and Prkar1a knock-out SCs. ***G***, Prkar1a knock-out cells stained with SC markers S100β or P75NTR. ***H***, PKA inhibitor PKI treatment partially rescued abnormal cell morphology in Prkar1a knock-out cultures. ***I***, Prkar1a knock-out SCs contain fewer lamellipodia (arrow) compared with control cells. $n = 60$ cells from three independent experiments (*$p < 0.05$, ***$p < 0.001$; one-way ANOVA followed by Tukey's *post hoc* test). Error bars indicate ± SEM. Scale bars: ***A***, ***C***, 100 μM.

creased SC proliferation in Prkar1a-SCKO nerves *in vivo*. In Prkar1a-SCKO SCs sorted into 1:1 relationships with axons *in vivo*, myelination began prematurely, correlating with an increase in a cAMP-regulated transcription factor Oct-6 expression and increased MBP expression.

The absence of Prkar1a regulatory subunits is predicted to unleash PKA catalytic subunits, resulting in high PKA activity during SC development *in vivo*. We confirmed a two-fold increase in PKA activity in Prkar1a-KO SCs. Consistent with effects of Prkar1a loss causing high PKA activity and cell phenotypes, we were able to partially reverse some abnormalities in Prkar1a-KO cells with a weak inhibitor of PKA, PKI (Guergnon et al., 2006).

The high expression of the Oct6 transcription factor in Prkar1a mutant nerves provides additional evidence that PKA activity is upregulated in the mutant nerves. We therefore infer that high cAMP/PKA signaling in Prkar1a-SCKO SC inhibited SC proliferation *in vivo*, and that high cAMP/PKA activity negatively regulates SC proliferation. Consistent with our results, at low levels of cAMP activation, the SC mitogen NRG1 promotes SC proliferation, whereas a higher concentration of cAMP reduced SC proliferation and promoted differentiation (Arthur-Farraj et al., 2011). In addition, infection of SCs with dominant negative PKA effectively blocked forskolin-stimulated SC mitosis (Howe and McCarthy, 2000). However, we cannot formally exclude Prkar1a

functions outside the PKA holoenzyme in the phenotypes we describe.

The abnormal multiple processes we identified in Prkar1a-SCKO SCs are caused at least in part by high PKA activity in Prkar1a knock-out SCs because the PKA inhibitor PKI substantially prevented the occurrence of this phenotype. However, neither reduced lamellipodia formation in Prkar1a-SCKO SCs nor SC growth were rescued by the weak PKA inhibitor PKI (data not shown). It is possible that precise levels of PKA might rescue function. It is likely that highly regulated levels of PKA are necessary at precise times in development to coordinate radial sorting with SC proliferation and differentiation and maintain the balance between SC proliferation and differentiation *in vivo*, as predicted by *in vitro* studies.

Supporting the idea that Prkar1a is relevant in SCs, inactivating mutations in *PRKAR1A* are found in patients with Carney complex (CNC; Kirschner et al., 2000), some of whom develop peripheral nerve tumors, schwannomas (Stratakis, 2002; Stergiopoulos and Stratakis, 2003). Indeed, mice heterozygous for Prkar1a mutations or those with tissue-specific ablation in subset of mouse cranial neural crest cells developed schwannomas (Kirschner et al., 2005; Jones et al., 2008). In contrast to our observation that Prkar1a loss reduces SC proliferation when expressed beginning at the SC precursor stage of development, specific knock-out of *Prkar1a* in a subset of mouse facial neural crest cells increased SCs proliferation and induced schwannoma formation (Jones et al., 2008). These intriguing data suggest that either PKA activity has opposite effects on SC proliferation in different developmental cell contexts and/or that additional genetic events are necessary to promote tumorigenesis in Carney complex.

Our data reveal a previously unknown function of Prkar1a in SC radial sorting. In part, the observed failure of radial sorting may be secondary to decreased SC numbers in Prkar1a-SCKO nerves. We believe that it is likely that additional factors also contribute to the radial sorting defect, because SCs present in nerve failed to extend processes into axon bundles to segregate axons, and Prkar1a-SCKO SCs *in vitro* showed abnormal cell morphology. These *in vitro* morphology changes correlate with failure of SC radial sorting in the Prkar1a-SCKO nerves. Cell morphology is largely controlled by remodeling of the actin cytoskeleton through Rho GTPases, GTP-binding proteins (Rho, Rac, and cdc42) that activate downstream kinases when GTP-bound. Each of the Rho family GTPases has been implicated in aspects of axonal sorting, SC proliferation and/or myelination (Melendez-Vasquez et al., 2004; Feltri et al., 2008; Krause et al., 2008). In the absence of Prkar1a, it is plausible that active PKA phosphorylates proteins that regulate Rho signaling. Rac1 activity was upregulated in SCs when Prkar1a was ablated in neural crest cells (Jones et al., 2008; Manchanda et al., 2013). PKA phosphorylates GTP dissociation inhibitor to negatively regulate Rho activity (Qiao et al., 2008), and can directly phosphorylate Rho (Jones and Palmer, 2012). PKA phosphorylates the Rac-GEF IQ-GAP2, enhancing Rac inactivation (Logue et al., 2011). Cdc42 might also be involved, as PKA can result in translocation of the exchange factor β1-PIX and Cdc42 activation (Chahdi et al., 2005).

The expression of Oct6, an important transcription factor in SC myelination, was dramatically increased in Prkar1a-SCKO nerves. Oct6 was expressed in all nerve SCs consistent with a major role for PKA in regulation of Oct6 expression *in vivo*. The altered SC differentiation status (Oct6+;MBP+ or Oct6+; MBP−) of perinatal SCs may contribute to the observed failure

of axon sorting and decrease in cell proliferation. Notably, although expression of MBP was accelerated in Prkar1a-SCKO nerves, only a few myelin sheaths formed early in Prkar1a-SCKO sciatic nerves, although this did not translate into presence of large numbers of myelinated fibers in a rare Prkar1a-SCKO nerve analyzed at P25. We were unable to generate mice to determine whether Oct6 expression persists past the perinatal period in Prkara1a-SCKO nerves, but our results are consistent with a study showing that persistent Oct6 expression can result in hypomyelination (Ryu et al., 2007).

It is likely that highly regulated levels of PKA coordinate radial sorting with SC proliferation and differentiation. In particular, precise levels of cAMP are likely to maintain the balance between SC proliferation and differentiation *in vivo*, as predicted by *in vitro* studies. In this context, it will be interesting to test whether SC proliferation is increased in Gpr126 knock-out mice or Rac1-CKO mice that have low cAMP/PKA signaling (Monk et al., 2011; Guo et al., 2012). In conclusion, we have identified a critical role for the R1a subunit of PKA in regulation of peripheral nerve SC development. Prkar1a controls process extension by SCs and radial sorting in nerve development, as well as SC numbers and timing of expression of myelin genes in peripheral nerves.

References

Amieux PS, Howe DG, Knickerbocker H, Lee DC, Su T, Laszlo GS, Idzerda RL, McKnight GS (2002) Increased basal cAMP-dependent protein kinase activity inhibits the formation of mesoderm-derived structures in the developing mouse embryo. J Biol Chem 277(30):27294–27304. CrossRef Medline

Arthur-Farraj P, Wanek K, Hantke J, Davis CM, Jayakar A, Parkinson DB, Mirsky R, Jessen KR (2011) Mouse schwann cells need both NRG1 and cyclic AMP to myelinate. Glia 59:720–733. CrossRef Medline

Barradeau S, Imaizumi-Scherrer T, Weiss MC, Faust DM (2002) Intracellular targeting of the type-I alpha regulatory subunit of cAMP-dependent protein kinase. Trends Cardiovasc Med 12:235–241. CrossRef Medline

Bossis I, Stratakis CA (2004) Minireview: PRKAR1A: normal and abnormal functions. Endocrinology 145:5452–5458. CrossRef Medline

Chahdi A, Miller B, Sorokin A (2005) Endothelin 1 induces beta 1Pix translocation and Cdc42 activation via protein kinase A-dependent pathway. J Biol Chem 280:578–584. CrossRef Medline

Cheng X, Ji Z, Tsalkova T, Mei F (2008) Epac and PKA: a tale of two intracellular cAMP receptors. Acta Biochim Biophys Sin (Shanghai) 40:651–662. CrossRef Medline

Davis JB, Stroobant P (1990) Platelet-derived growth factors and fibroblast growth factors are mitogens for rat Schwann cells. J Cell Biol 110:1353–1360. CrossRef Medline

Feltri ML, Suter U, Relvas JB (2008) The function of RhoGTPases in axon ensheathment and myelination. Glia 56:1508–1517. CrossRef Medline

Guergnon J, Dessauge F, Traincard F, Cayla X, Rebollo A, Bost PE, Langsley G, Garcia J (2006) A PKA survival pathway inhibited by DPT-PKI, a new specific cell permeable PKA inhibitor, is induced by *T. annulata* in parasitized B-lymphocytes. Apoptosis 11:1263–1273. CrossRef Medline

Guo L, Moon C, Niehaus K, Zheng Y, Ratner N (2012) Rac1 controls Schwann cell myelination through cAMP and NF2/merlin. J Neurosci 32:17251–17261. CrossRef Medline

Howe DG, McCarthy KD (2000) Retroviral inhibition of cAMP-dependent protein kinase inhibits myelination but not Schwann cell mitosis stimulated by interaction with neurons. J Neurosci 20:3513–3521. Medline

Jaegle M, Ghazvini M, Mandemakers W, Piirsoo M, Driegen S, Levavasseur F, Raghoenath S, Grosveld F, Meijer D (2003) The POU proteins brn-2 and oct-6 share important functions in Schwann cell development. Genes Dev 17:1380–1391. CrossRef Medline

Jessen KR, Mirsky R (1997) Embryonic Schwann cell development: the biology of Schwann cell precursors and early Schwann cells. J Anat 191:501–505. Medline

Jessen KR, Mirsky R (1991) Schwann cell precursors and their development. Glia 4:185–194. CrossRef Medline

Jessen KR, Mirsky R (2005) The origin and development of glial cells in peripheral nerves. Nat Rev Neurosci 6:671–682. CrossRef Medline

Jones GN, Tep C, Towns WH 2nd, Mihai G, Tonks ID, Kay GF, Schmalbrock PM, Stemmer-Rachamimov AO, Yoon SO, Kirschner LS (2008) Tissue-specific ablation of Prkar1a causes schwannomas by suppressing neurofibromatosis protein production. Neoplasia 10:1213–1221. CrossRef Medline

Jones SE, Palmer TM (2012) Protein kinase A-mediated phosphorylation of RhoA on serine 188 triggers the rapid induction of a neuroendocrine-like phenotype in prostate cancer epithelial cells. Cell Signal 24:1504–1514. CrossRef Medline

Jung-Testas I, Schumacher M, Bugnard H, Baulieu EE (1993) Stimulation of rat Schwann cell proliferation by estradiol: synergism between the estrogen and cAMP. Brain Res Dev Brain Res 72:282–290. CrossRef Medline

Kim HA, DeClue JE, Ratner N (1997) cAMP-dependent protein kinase A is required for Schwann cell growth: interactions between the cAMP and neuregulin/tyrosine kinase pathways. J Neurosci Res 49:236–247. CrossRef Medline

Kirschner LS (2009) Use of mouse models to understand the molecular basis of tissue-specific tumorigenesis in the Carney complex. J Intern Med 266:60–68. CrossRef Medline

Kirschner LS, Carney JA, Pack SD, Taymans SE, Giatzakis C, Cho YS, Cho-Chung YS, Stratakis CA (2000) Mutations of the gene encoding the protein kinase A type I-alpha regulatory subunit in patients with the Carney complex. Nat Genet 26:89–92. CrossRef Medline

Kirschner LS, Kusewitt DF, Matyakhina L, Towns WH 2nd, Carney JA, Westphal H, Stratakis CA (2005) A mouse model for the Carney complex tumor syndrome develops neoplasia in cyclic AMP-responsive tissues. Cancer Res 65:4506–4514. CrossRef Medline

Krause S, Stendel C, Senderek J, Relvas JB, Suter U (2008) Small rho GTPases are key regulators of peripheral nerve biology in health and disease. J Peripher Nerv Syst 13:188–199. CrossRef Medline

Logue JS, Whiting JL, Tunquist B, Langeberg LK, Scott JD (2011) Anchored protein kinase A recruitment of active rac GTPase. J Biol Chem 286:22113–22121. CrossRef Medline

Madisen L, Zwingman TA, Sunkin SM, Oh SW, Zariwala HA, Gu H, Ng LL, Palmiter RD, Hawrylycz MJ, Jones AR, Lein ES, Zeng H (2010) A robust and high-throughput Cre reporting and characterization system for the whole mouse brain. Nat Neurosci 13:133–140. CrossRef Medline

Manchanda PK, Jones GN, Lee AA, Pringle DR, Zhang M, Yu L, La Perle KM, Kirschner LS (2013) Rac1 is required for Prkar1a-mediated Nf2 suppression in Schwann cell tumors. Oncogene, in press. CrossRef Medline

Melendez-Vasquez CV, Einheber S, Salzer JL (2004) Rho kinase regulates schwann cell myelination and formation of associated axonal domains. J Neurosci 24:3953–3963. CrossRef Medline

Monje PV, Bartlett Bunge M, Wood PM (2006) Cyclic AMP synergistically enhances neuregulin-dependent ERK and akt activation and cell cycle progression in Schwann cells. Glia 53:649–659. CrossRef Medline

Monk KR, Naylor SG, Glenn TD, Mercurio S, Perlin JR, Dominguez C, Moens CB, Talbot WS (2009) A G-protein-coupled receptor is essential for Schwann cells to initiate myelination. Science 325:1402–1405. CrossRef Medline

Monk KR, Oshima K, Jörs S, Heller S, Talbot WS (2011) Gpr126 is essential for peripheral nerve development and myelination in mammals. Development 138:2673–2680. CrossRef Medline

Monuki ES, Weinmaster G, Kuhn R, Lemke G (1989) SCIP: a glial POU domain gene regulated by cyclic AMP. Neuron 3:783–793. CrossRef Medline

Morgan L, Jessen KR, Mirsky R (1991) The effects of cAMP on differentiation of cultured Schwann cells: progression from an early phenotype (04+) to a myelin phenotype (P0+, GFAP−, N-CAM−, NGF-receptor−) depends on growth inhibition. J Cell Biol 112:457–467. CrossRef Medline

Pereira JA, Lebrun-Julien F, Suter U (2012) Molecular mechanisms regulating myelination in the peripheral nervous system. Trends Neurosci 35:123–134. CrossRef Medline

Qiao J, Holian O, Lee BS, Huang F, Zhang J, Lum H (2008) Phosphorylation of GTP dissociation inhibitor by PKA negatively regulates RhoA. Am J Physiol Cell Physiol 295:C1161–C1168. CrossRef Medline

Ryu EJ, Wang JY, Le N, Baloh RH, Gustin JA, Schmidt RE, Milbrandt J (2007) Misexpression of Pou3f1 results in peripheral nerve hypomyelination and axonal loss. J Neurosci 27:11552–11559. CrossRef Medline

Skalhegg BS, Tasken K (2000) Specificity in the cAMP/PKA signaling pathway: differential expression, regulation, and subcellular localization of subunits of PKA. Front Biosci 5:D678–D6793. CrossRef Medline

Sobue G, Shuman S, Pleasure D (1986) Schwann cell responses to cyclic AMP: proliferation, change in shape, and appearance of surface galactocerebroside. Brain Res 362:23–32. CrossRef Medline

Stergiopoulos SG, Stratakis CA (2003) Human tumors associated with Carney complex and germline PRKAR1A mutations: a protein kinase A disease! FEBS Lett 546:59–64. CrossRef Medline

Stewart HJ, Eccleston PA, Jessen KR, Mirsky R (1991) Interaction between cAMP elevation, identified growth factors, and serum components in regulating Schwann cell growth. J Neurosci Res 30:346–352. CrossRef Medline

Stewart HJ, Morgan L, Jessen KR, Mirsky R (1993) Changes in DNA synthesis rate in the Schwann cell lineage in vivo are correlated with the precursor: Schwann cell transition and myelination. Eur J Neurosci 5:1136–1144. CrossRef Medline

Stratakis CA (2002) Mutations of the gene encoding the protein kinase A type I-alpha regulatory subunit (PRKAR1A) in patients with the "complex of spotty skin pigmentation, myxomas, endocrine overactivity, and schwannomas" (Carney complex). Ann N Y Acad Sci 968:3–21. CrossRef Medline

Taylor SS, Kim C, Vigil D, Haste NM, Yang J, Wu J, Anand GS (2005) Dynamics of signaling by PKA. Biochim Biophys Acta 1754:25–37. CrossRef Medline

Williams JP, Wu J, Johansson G, Rizvi TA, Miller SC, Geiger H, Malik P, Li W, Mukouyama YS, Cancelas JA, Ratner N (2008) Nf1 mutation expands an EGFR-dependent peripheral nerve progenitor that confers neurofibroma tumorigenic potential. Cell Stem Cell 3:658–669. CrossRef Medline

Woodhoo A, Sommer L (2008) Development of the Schwann cell lineage: from the neural crest to the myelinated nerve. Glia 56:1481–1490. CrossRef Medline

Wu J, Williams JP, Rizvi TA, Kordich JJ, Witte D, Meijer D, Stemmer-Rachamimov AO, Cancelas JA, Ratner N (2008) Plexiform and dermal neurofibromas and pigmentation are caused by Nf1 loss in desert hedgehog-expressing cells. Cancer Cell 13:105–116. CrossRef Medline

Yin Z, Jones GN, Towns WH 2nd, Zhang X, Abel ED, Binkley PF, Jarjoura D, Kirschner LS (2008) Heart-specific ablation of Prkar1a causes failure of heart development and myxomagenesis. Circulation 117:1414–1422. CrossRef Medline

Yoon C, Korade Z, Carter BD (2008) Protein kinase A-induced phosphorylation of the p65 subunit of nuclear factor-kappaB promotes Schwann cell differentiation into a myelinating phenotype. J Neurosci 28:3738–3746. CrossRef Medline